Proceedings of DETC'02
ASME 2002 Design Engineering Technical Conferences
and Computers and Information in Engineering Conference
Montreal, Canada, September 29 - October 2, 2002

DETC2002/DAC-34129

NEW CONCEPTS IN GRAPHIC VISUALIZATION OF OBJECTIVE FUNCTIONS

Petru-Aurelian Simionescu
Auburn University
Department of Mechanical Engineering
202 Ross Hall
Auburn, Al 36849

David G. Beale
Auburn University
Department of Mechanical Engineering
201 Ross Hall
Auburn, Al 36849

ABSTRACT

A method of inspecting the design space of multivariable objective functions is proposed. By scanning 1 or 2 of the variables at a constant step while partially minimizing or maximizing the function with respect to the remaining variables, sets of points are generated that can be further used in producing 2D or 3D diagrams. A number of examples are given for showing the usefulness of the method in studying the design space of objective functions and of the constraint activity. All graphs are produced with an in-house program that allows generation of logarithmically spaced level-curve diagrams and accurately truncating function surfaces over the z-axis at specified heights.

INTRODUCTION

Functions of one variable $f(x)$ can be straightforwardly represented in the 2D paper space where one dimension can be associated with the variable and the other dimension with the function value. As an extension, functions of two variables $f(x_1, x_2)$ can be visualized as families of curves x_1=constant, x_2=constant or z=constant (also called level curve diagrams). Another possibility is to plot the $z=f(x_1, x_2)$ surface, which is equally intuitive since of the 3D Euclidean space, two dimensions can be associated with x_1 and x_2 and the third dimension with the function value. Numerous mathematical and operations research publications give examples of such representations, which allow for a better understanding of the properties of the respective functions, such as: monotonicity, convexity, smoothness, the existence of multiple minima, constraint activity etc.

Functions of three variables can also be represented graphically, like plotting the relative proportions of three ingredients in a mixture [1] (although the 3 variables are not independent because the proportions sum must be unity). Other methods employing multiple-color plots and computer animation are described by Encarnação et al [2] and Jones [3]. One example of scanning two of the variables through a number of 3D representations generated for different values of the third variable in the case of a $f(x_1, x_2, x_3)$ function is available in [4]. It is obvious that the number of plots required for visualizing the same way functions of more than three variables is prohibitively large, and the method becomes ineffective (following the approach described in [4], where 15 surface plots were used for inspecting the design space of a function of 3 variables, a 4-variable objective function would require 15^2=225 representations, and a 5-variable objective function 15^3=3375 representations).

In the field of artificial neural networks, in particular, have been proposed numerous techniques for the visualization of the multidimensional spaces in both the learning process and the prediction process [5-7]. Fluid flow data, radar range images, atmospheric and oceanographic measurements also generate large multidimensional, multivariate data sets, the visualization of which continues to be an active and promising research area [8]. The interested reader is suggested to visit the Web site: http://catt.bus.okstate.edu/jones98/ for an exhaustive list of publication on the use of visualization to support optimisation modelling, solution and analysis.

In the present paper a method of inspecting graphically the design space of multivarite objective functions $F(x_1 \ldots x_n)$, for which the configurations of the minimum domains are particularly of interest, will be presented. Since $min F=-max(-F)$, only functions for which the optimum sought is a minimum will be discussed. The main idea of the method is to perform partial minimizations of the function with respect to all but 1 or 2 of the design variables, and to generate an appropriate number point-sets that will be further used for producing 2D or 3D graphical representations.

METHOD DESCRIPTION

Consider a multivariable objective functions $F(x_1 \ldots x_n)$ with $x_i \in [x_{i\min}..x_{i\max}]$ (i=1..n, $n \geq 2$) variables' domains, not necessarily side constraints. One of the variables, for example x_1, can be scanned with a constant step in-between the limits $[x_{1\min}..x_{1\max}]$ and a minimization of F performed with respect to the remaining variables $x_2..x_n$. In the following x_1 will be named *state variable* while $x_2 \ldots x_n$ will be named *free variable* and the following one-variable partial-minima function defined:

$$G_{2..n}(x_1) = \min_{x_2 \ldots x_n} F(x_1 \ldots x_n) \tag{1}$$

By generating successive sets of points $[x_1, G_{2..n}(x_1)]$ for $x_1 \in [x_{1\min}..x_{1\max}]$, this function can be very conveniently represented graphically. In total, n such diagrams can be generated, equal to the number of variables of the objective function.

Similarly, if 2 of the variables (for example x_1 and x_2) are considered state variables, a two-variable partial-minima function can be defined:

$$G_{3..n}(x_1, x_2) = \min_{x_3 \ldots x_n} F(x_1 \ldots x_n) \tag{2}$$

which the same can be represented graphically as level curve or 3D surface diagram, for some chosen limits $[x_{1\min}..x_{1\max}]$ and $[x_{2\min}..x_{2\max}]$. In this case a total of $C(n,2)=n(n-1)/2$ diagrams can be produced.

It will be further shown that graphical representations of the partial-minima functions can give a good feeling of the properties of the original objective function F, particularly if a number of representations are produced for different state variable(s) chosen from among the n design variables.

The authors agree that partial minimization is not a totally new concept: Papalambros and Wilde [9] described the usefulness of partial minimization with respect to only one of the variables, while the remaining n-1 variables have been assigned arbitrary fix values, for inspecting the design space of objective functions and studying the constraint activity. Also design studies, commonly used in practice, imply scanning one of the parameters while maintaining constant the remaining ones. It is however believed to be the first time when minimization is performed with respect to all but 1 or 2 of the variables of the objective function and the resultant partial minima used for graphical representation purposes.

As compared to [4] or to the one-dimensional partial minimization explained by Papalambros and Wilde [9], where the global minima is unlikely to be identified, the proposed method has the advantage that the global minima will always show on the diagram (under the condition that the domains of the state variables includes this point, and that the searching subroutine has global searching capabilities). If the function is multimodal, the existence of more than one minima will also be revealed. Evidently, the precision with which the minimum point(s) are shown on the graph will be dependent to the resolution with which the state variable interval(s) have been discretized.

Any tangent discontinuities and curvature change of the graph (other then those caused by premature convergences of the searching algorithm that will appear in a irregular pattern) are a sign of the original objective function being nonsmooth, multimodal or of some of the constraints changing their activity.

If in a similar manner a *partial maximizations* of the objective function is performed, the upper limits of the function value can be determined, which together with the already found lower limits, can aid in scaling the design variables. This partial maximization has sense only when the global maxima of the function is less than infinity.

Finally, in case of constrained optimization problems, the proposed visualization method allows for a very suggestive revealing of the constraint activity, by comparing the partial-minima graph(s) of the objective function with similar graphs generated for some or all of the constraints suspended.

The usefulness of the presented techniques will be best emphasized considering a number of optimization problems of both unconstrained and constrained objective functions taken from engineering and operations research literature.

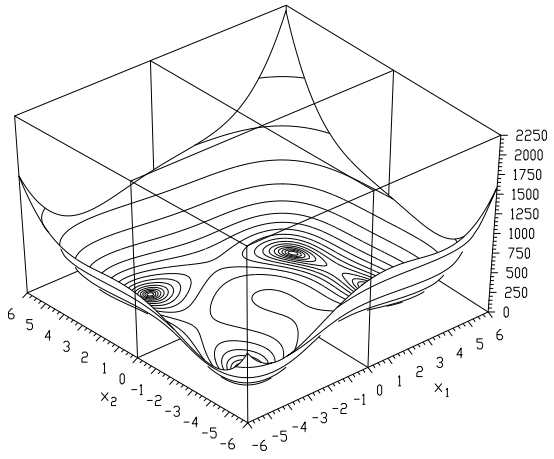

Fig. 1 Rise level curve plot of Himmelblau function (F1).

NUMERICAL EXAMPLES

Example 1: In order to clarify ideas, the first example considered is that of a two-variable objective function:

$$F1(x_1, x_2) = (x_1^2 + x_2 - 11)^2 + (x_1 + x_2^2 - 7)^2 \tag{3}$$

known as Himmelblau function [10], that can be directly visualized in the 3D space (see Fig. 1). The graphical representation of this function shows clearly the existence of 4 local minima. This same property can be revealed if the following one-variable-partial-minima functions are studied:

$$G1_2(x_1) = \min_{x_2} F1(x_1, x_2) \tag{4}$$

and

$$G1_1(x_2) = \min_{x_1} F1(x_1, x_2)\,. \tag{5}$$

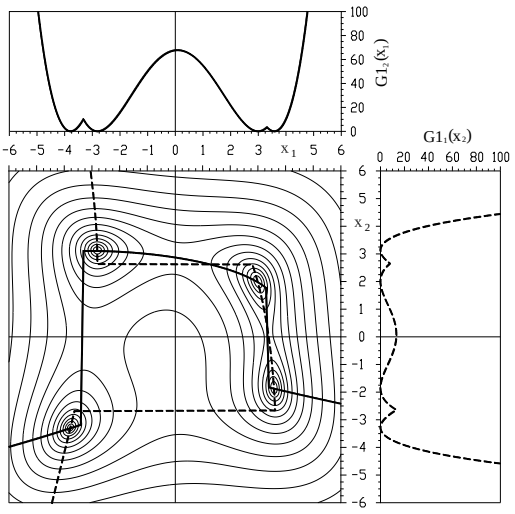

Fig. 2 Contour plot of Himmelblau function (middle) and plots of partial minima functions $G1_2(x_1)$ (above) and $G1_1(x_2)$ (right). Also shown are the graphs of the minimum values of x_2 and x_1 as they result when evaluating the respective functions $G1_2$ and $G1_1$.

The graphs of $G1_2(x_1)$ and $G1_1(x_2)$ are shown in Fig. 2 (above and to the right of the level curve diagram of F1). It can be seen that the same as (3), these two functions feature a total of 4 local minima. The partial minimizations required to generate the graphs of $G1_1$ and $G1_2$ have been performed using Brent's algorithm [11] preceded by a 200-division grid search to ensure finding the successive global partial minima and not some local minima.

Superimposed to the level curve diagram of F1 in Fig. 2, are the graphs of the optimum values of x_1 and x_2 as they result in the partial minimization process when evaluating $G1_1$ and $G1_2$. They are paths on the $z=F1(x_1, x_2)$ surface which projected on x_1=constant or x_2=constant vertical planes result in the graphs of $G1_1(x_1)$ and $G1_2(x_2)$ respectively. In turn these

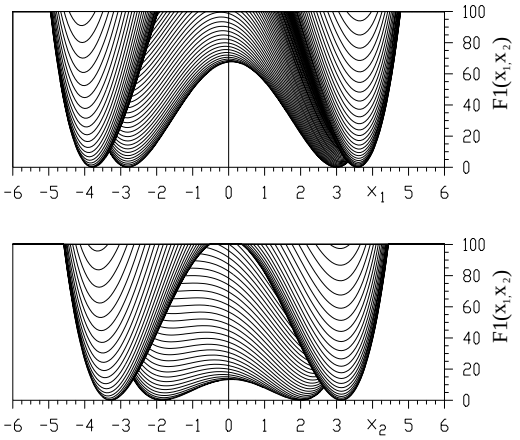

Fig. 3 Side views of the lower part of $F1(x_1,x_2)$ truncated at z=100, to be compared with the graphs of $G1_2(x_1)$ and $G1_1(x_2)$ in Fig. 2, respectively.

graphs can be seen as *silhouettes* of the lowest points of $F1(x_1,x_2)$ in side view (see Fig. 3).

For objective functions of n variables with n>2, this intersection or projection/silhouette analogy is less intuitive because the function is geometrically equivalent to an n-hypersurface that cannot be represented graphically directly. However, three-dimensional and two-dimensional intersections on such hypersurfaces (i.e. 3D surfaces and projected curves) can be visualized in the 3D Euclidean space as will be further shown. One-dimensional intersections (i.e. single points - notably points of minima or maxima) also deserve attention, but they can be simply specified by their coordinates.

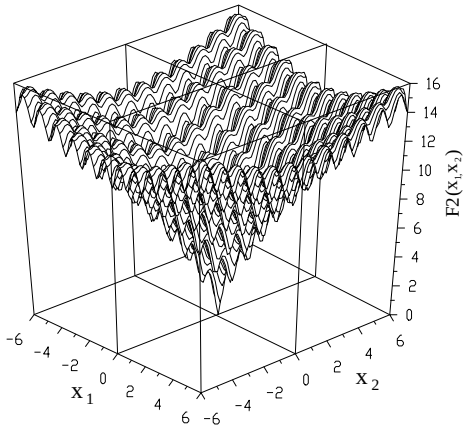

Fig. 4 Surface plot of the two-dimensional variant of F2.

Example 2: The first multivariate objective function considered was Ackley's function:

$$F2(x_1 \ldots x_n) = 20\left[1 - \exp\left(-\frac{1}{2}\sqrt{\frac{1}{n}\sum_{i=1}^{n} x_i^2}\right)\right] - \exp\left(\frac{1}{n}\sum_{i=1}^{n}\cos(2\pi x_i)\right) + e \qquad (6)$$

This is considered a highly multimodal objective function commonly used in rating genetic algorithms [12]. Irrespective of n, its global minima equals 0, and occurs for $x_1=x_2=\ldots x_n=0$. A plot of F2 for the case of n=2 is shown in Fig. 4. In order to investigate the properties of Ackley's function of more than 2 variables $[x_1, x_2, G2_{3..n}(x_1, x_2)]$ triplets were generated with:

$$G2_{3..n}(x_1, x_2) = \min_{x_3..x_n} F2(x_1 \ldots x_n). \qquad (7)$$

for the case of n=30, and the diagram in Fig. 5 plotted. The subroutine used for the successive evaluation of $G2_{3..n}$ combines a genetic algorithm named ***3P*** described elsewhere [13] and the Simplex method due to Nealder and Mead [14]. For all partial minima thus calculated, the corresponding free variables prove to have the same value i.e. $x_3=x_4=..x_n=0$. This implies that the analytic expression of (7) writes:

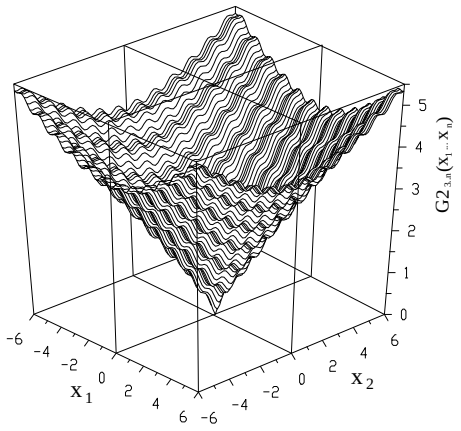

Fig. 5 Surface plot of partial-minima function of F2 with respect to $x_3, x_4, ..x_n$, for the case of n=30.

$$G2_{3..n}(x_1, x_2) = 20\left[1 - \exp\left(-\frac{1}{5}\sqrt{\frac{x_1^2 + x_2^2}{n}}\right)\right] - \exp\left(\frac{\cos(2\pi x_1) + \cos(2\pi x_2) - 2}{n} + 1\right) + e \quad (8)$$

which explains the resemblance of this latter graph and the graph of F2 for n=2 in Fig. 4.

Interesting conclusions were further derived by graphically displaying the following partial-minima function:

$$G2_{2..n}(x_1) = \min_{x_2..x_n} F2(x_1...x_n) = 20\left[1 - \exp\left(-\frac{1}{5}\sqrt{\frac{x_1^2}{n}}\right)\right] - \exp\left(\frac{\cos(2\pi x_1) - 1}{n} + 1\right) + e \quad (9)$$

for various values of n respectively, together with the n=1 variant of (6). Their combined graphs shown in Fig. 6 reveal that as n increases, Ackley's function smoothens, flattens to zero and becomes unimodal, contradicting the common belief that as n increases, this function is more difficult to minimize.

Because $F2(x_1..x_n)$ is homogenous with respect to all variables, it implies that choosing any state variables will result

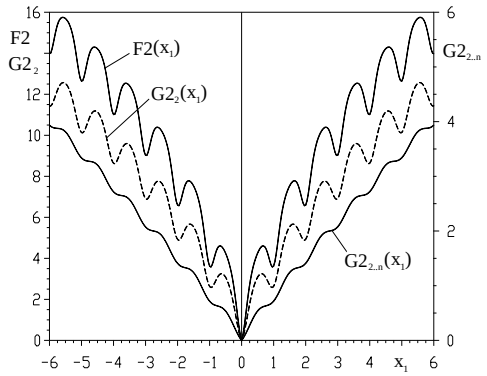

Fig. 6 Combined graph of $F2(x_1)$, $G2_2(x1)$ and $G2_{2..n}(x1)$ with n=30.

in identical analytical expressions and diagrams of the partial minima functions (8) and (9). These and the previous conclusions, now evident, are however less obvious without performing the partial minimizations and graphical representations described above.

Example 3: One example of a constrained objective function considered is (problem 4 in [15]):

$$F3(x_1...x_7) = 0.7854 \cdot x_1 \cdot x_2^3(3.3333 \cdot x_3^2 + 14.9334 \cdot x_3 - 43.0934) - 1.508 \cdot x_1(x_6^2 + x_7^2) + 0.7477(x_6^3 + x_7^3) + 0.7854(x_4 \cdot x_6^2 + x_5 \cdot x_7^2)$$

$$\text{subjected to:} \quad (10)$$

$$2.6 \le x_1 \le 3.6$$

$$0.7 \le x_2 \le 0.8 \qquad 17 \le x_2 \le 28$$

$$7.3 \le x_4 \le 8.3 \qquad 7.3 \le x_5 \le 8.3$$

$$2.9 \le x_6 \le 3.9 \quad \text{and} \quad 5 \le x_2 \le 5.5$$

the minimum of which equals 2352.448 and occurs for x_1=2.6, x_2=0.7, x_3=17, x_4=7.3, x_5=7.3, x_6=2.9, x_7=5. This property is visible from the graphs of partial minima of F3 with respect to x_2, x_3, x_4, x_5, x_6 (Fig. 7-a) and to x_1, x_2, x_3, x_6, x_7 (Fig. 8-a). In both cases the values of the free variables converged during the minimization process to their lowest admissible values, a confirmation that at minimum all constraints are active.

In order to get an idea about the range the function value can experience, a maximization of F3 was also performed, and the graphs of:

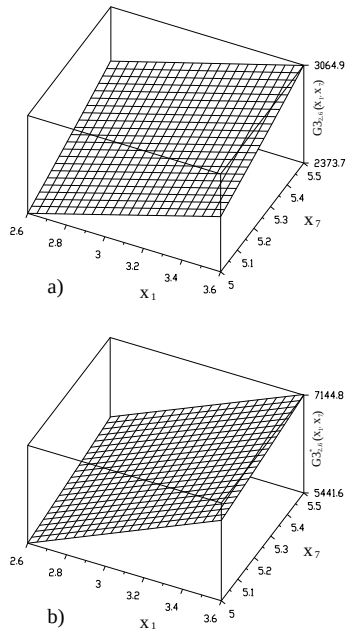

Fig. 7 Surface plots of the test objective function F3 (**a**) partially minimized and (**b**) partially maximized with respect to x_2, x_3, x_4, x_5 and x_6.

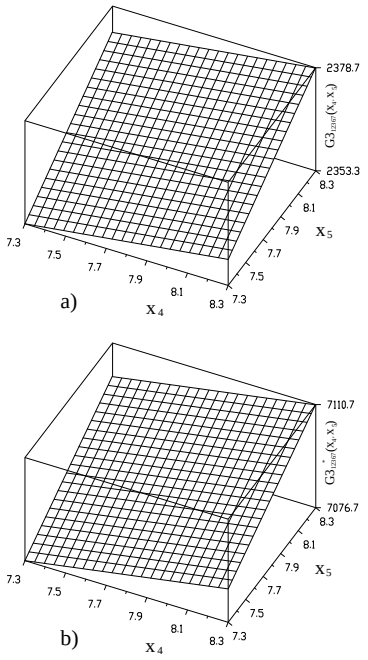

Fig. 8 Surface plots of the test objective function F3, (**a**) partially minimized and (**b**) partially maximized with respect

$$G3^{*}_{23456}(x_1, x_7) = \max_{x_2 x_3 x_4 x_5 x_6} F3(x_1 \ldots x_7)$$
$$G3^{*}_{12367}(x_4, x_5) = \max_{x_1 x_2 x_3 x_6 x_7} F3(x_1 \ldots x_7) \quad (11)$$

in Fig. 7-b and Fig. 8-b generated. Together with the plots of partial minima, such diagrams can prove useful in various design studies or in chosing appropriate scaling factors for the variables.

The search for the partial minima and partial maxima of F3 used in generating the diagrams in Figs. 7 and 8 was done using the same procedure that combines the 3P genetic algorithm and Nelder and Mead's Simplex algorithm. The constraints were introduced in the optimization problem using exterior penalty functions with very large penalty factors [16].

Example 4: The last test objective function is problem 5 in [15]:

$$F4(x_1, x_2, x_3) = (x_1^2 + x_2^2 + x_3^2)/2 - (x_1 + x_2 + x_3)$$
$$\text{subjected to:}$$
$$x_1 + x_2 + x_3 - 1 \le 0 \quad (12)$$
$$4x_1 + 2x_2 - 7/3 \le 0$$
$$x_1 \ge 0; \quad x_2 \ge 0 \quad \text{and} \quad x_3 \ge 0.$$

Its minimum equals -5/6 and is located in the point (1/3,1/3,1/3) for which the constraint $x_1+x_2+x_3-1\le 0$ is active.

Using Brent's algorithm, all possible partial-minima diagrams have been generated (Figs. 9-a, 10-a, 11-a). The values of the free variable corresponding to these partial

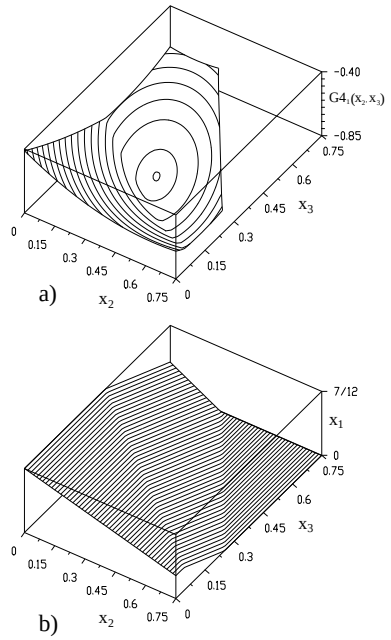

Fig. 9 Contour plot of the test objective function F4 (**a**) partially minimized with respect to x_1 and (**b**) the diagram of the corresponding values of x_1.

minima have also been recorded and the plots in Figs. 9-b, 10-b and 11-b generated. The constraint activity can be identified as lines of curvature discontinuity on both the partial minima and state variable diagrams.

From the graphical representation of $G4_1(x_2,x_3)$, $G4_2(x_1,x_3)$ and $G4_3(x_1,x_2)$, one would suppose that the global minimum of F_4 is

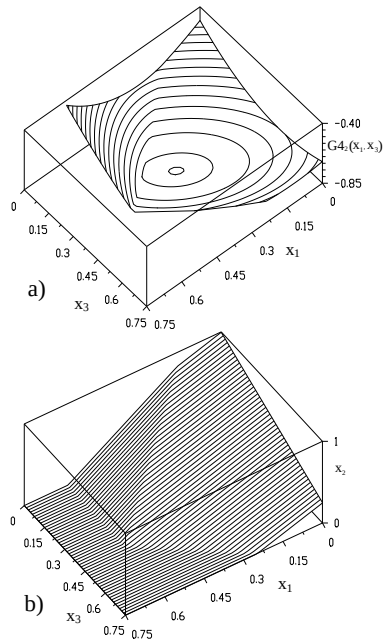

Fig. 10 Contour plot of the test objective function F4, (**a**) partially minimized with respect to x_2 and (**b**) the diagram of the corresponding values of x_2.

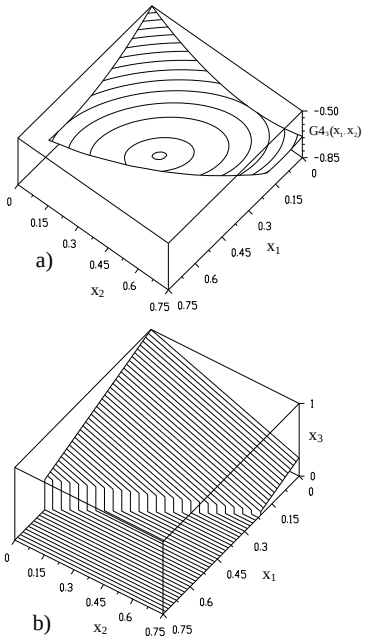

Fig. 11 Contour plot of the test objective function F4, (**a**) partially minimized with respect to x_3 and (**b**) the diagram of the corresponding values of x_3.

located inside the feasible domain. This is however a misleading appearance as proved by plotting the same diagrams with the constraints removed shown in Fig. 12 (due to the fact that F_4 is homogenous in its variables, all these diagrams are identical and depict a constant decrease in magnitude of partial minima with the increase in value of respective state variables).

In conclusion, a complete study of the constrained activity would require plotting the graphs of partial minima of the function with some or all of the constraints removed and the change in the appearance of these graphs observed.

FUNCTION VISUALIZATION TOOLS

All the diagrams in this paper were generated with an in-house program named ***D3D***, which has several features that facilitate objective function representations. One is the capability of generating logarithmically spaced level curve diagrams, either projected on the bottom plane, or mapped on the function surface. In this way the level curves are concentrated in the lower area of the function-surface thus revealing better the minimum domains. The benefit of this technique is illustrated in Fig. 13 where Rosenbrok's function [17] is represented as level curve diagram, with the level curves equally spaced (Fig. 13-a) and logarithmically spaced (Fig. 13-b). The relation used for calculating the height of the horizontal cutting plane that generates the *j* level curve was:

$$z_j = z_{min} + \exp\left[(j-1)\cdot \ln\frac{z_{max} - z_{min} + 1}{m-1}\right] - 1. \qquad (13)$$

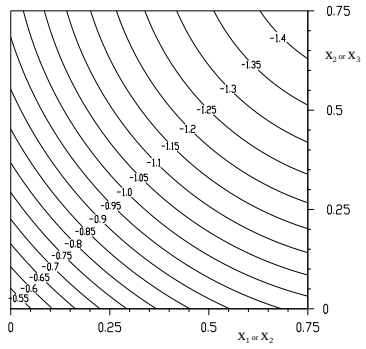

Fig. 12 Contour plot of $G4_1(x_2,x_3)$, $G4_2(x_1,x_3)$, $G4_3(x_1,x_2)$, with all the constraints removed.

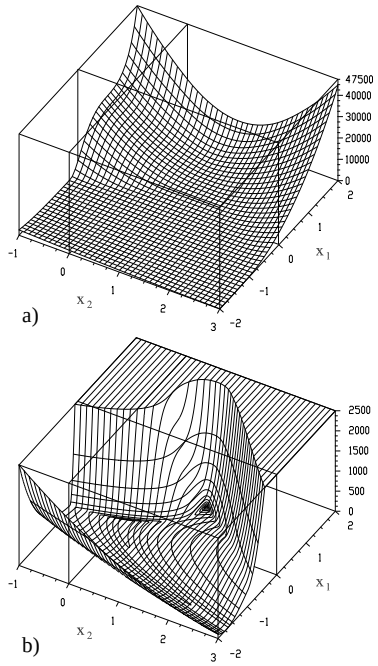

Fig. 14 Representation of the pseudo-objective function F5, (**a**) over its whole value range and (**b**) truncated over z to reveal the configuration of the minimum area domain. The occurrence of a second minima becomes now visible.

where *m* is the total number of level curves, and z_{min} and z_{max} are the minimum and maximum from among the heights used in sampling the function surface.

A second feature of *D3D* program, specially devised for visualizing penalized objective functions, is the possibility of trimming accurately the function surface over the *z*-axis. This feature is illustrated in Fig. 14 showing a plot of the pseudo-objective function:

$$F5(x_1, x_2) = 100 \cdot (x_2 - x_1^2)^2 + (x_1 - 1)^2 + 5000 \cdot \left(g_1^2 + g_2^2\right) \quad (14)$$

This is the same Rosenbrok's function, penalized with the following constrains:

$$g_1(x_1, x_2) = (x_1 - 1)^3 - x_2 + 1 \le 0$$
$$g_2(x_1, x_2) = x_1 + x_2 - 2 \le 0 \quad (15)$$

Within the chosen domain $-2 \le x_1 \le 2$ and $-1 \le x_2 \le 3$, the function value ranges from 0 to about 47500 (Fig. 14-a). As can be seen from Fig. 14-b by trimming the regions of the function surface exceeding 2500, a better insight into the domain of minimum can be obtained.

CONCLUSIONS

A suggestive technique for inspecting and visualizing the design space of objective functions arising in optimization problems have been presented. It requires partial minimization or maximization of the function with respect to all but 2 of the design variables and recording the resulting minima (together with the values of these *n*-2 variables), over a number of equally spaced points. Logarithmically spaced level curve diagrams and truncating the upper part of the graphs also facilitate revealing the properties of objective functions.

These repeated searches needed to generate the partial minimum diagrams in case of some properly chosen test objective functions, can be used to verify the speed and robustness of different optimization subroutines. If the plots of partial minima have spikes or sudden discontinuities, it is likely that the searching subroutine employed converged prematurely and its stop conditions must be revised or a more robust subroutine used.

The computation required for generating diagrams of partial minima can be very long in case of some objective functions, but with the advent of very high-speed personal computers, this is not a severe limitation. The procedure is well suited to parallel processing. Moreover, the CPU time can be notably reduced if the minimum found for one point on the diagram is used as initial guess for performing the search and generating the successive point.

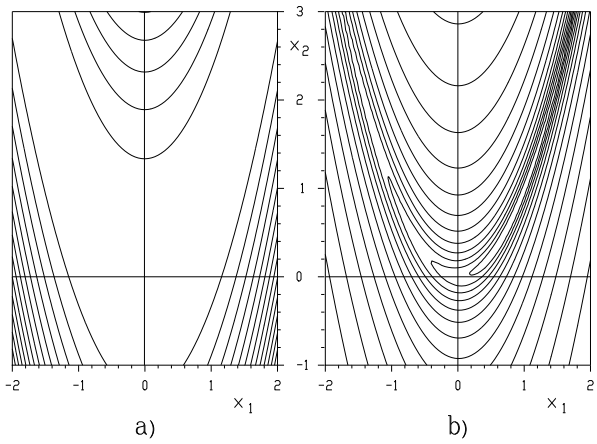

Fig. 13 Level-curve diagrams of Rosenbrok's function, (**a**) equally spaced and (**b**) logarithmically spaced.

REFERENCES:

[1] Devore, C.J., 2001, "Contour Plots for Three-Ingredient Mixing Problems," The Maple Application Center, http://www.mapleapps.com

[2] Encarnação, J.L., Lindner, R., Schlechtendahl, E.G., 1990, *Computer Aided Design. Fundamentals and System Architecture*, Springer-Verlag, Berlin, Heidelberg.

[3] Jones, C.V., 1996, *Visualization and Optimization*, Kluwer Academic Publishers.

[4] Kota, S., Chiou, S.J., 1993, "Use of Orthogonal Arrays in Mechanism Synthesis," Mechanism and Machine Theory, **28**, pp. 777-794.

[5] Hinton, G.E., Sejnowski, T.J., Ackley, D.H., 1984, "Boltzman Machines: Constraint Satisfaction Networks that Learn," Technical Report CMU-CS-84-119, Carnegie-Mellon University, Pittsburgh, PA.

[6] Wejchert, J., Tesauro, G., 1990, "Neural Network Visualization," in D. S. Touretzky, ed., *Advances in Neural Information Processing Systems*, Morgan Kaufmann, San Mateo, CA, pp. 465-472.

[7] Craven, M.W., Shavlik, J., 1991, "Visualization Learning and Computation in Artificial Neural Networks," International Journal of Artificial Neural Network Tools, **1**, pp. 399-425.

[8] Chen, J.X., Wang, S., 2001, "Data Visualization: Parallel Coordinates and Dimension Reduction," Computing in Science and Engineering, **5**, pp. 110–113.

[9] Papalambros, P.Y., Wilde, D.J., 2000, *Principles of Optimal Design: Modeling and Computation*, Cambridge University Press, UK.

[10] Himmelblau, D.M., 1972, *Applied Nonlinear Programming*, McGraw-Hill, New York.

[11] Brent, R.P., 1973 *Algorithms for Minimization Without Derivatives*, Prentice Hall.

[12] Yao, X., Liu, Y., Lin, G., 1999, "Evolutionary Programming Made Faster," IEEE Transactions on Evolutionary Computation, **3**, pp. 82-102.

[13] Simionescu, P.A., Beale, D., Overfelt, R.A., 2001, "Optimization of the Mold Orientation on an Investment Casting Centrifuge," *Proc. of the Artificial Neural Networks in Engineering Conference* (ANNE), St. Louis, MO, pp. 871-876
[14] Press, W.H., Flannery, B.P., Teukolsky, S., Vetterling, W.T., 1989, *Numerical Recipes*, Cambridge University Press, UK.
[15] Hansen, P., Jaumard, B., Lu, S. H., 1989, "Some Further Results on Monotonicity in Globally Optimal Design," ASME J. of Mechanisms, Transmissions and Automation in Design, **111**, pp. 345-352.
[16] Vanderplaats, G.N., 1984, *Numerical Optimization Techniques for Engineering Design*, McGraw-Hill.
[17] Rosenbrock, H.H., 1960, "An Automatic Method for Finding the Greatest or Least Value of a Function," Computer Journal **3**, pp. 175-184.